

Edge turbulence measurements in NSTX by gas puff imaging

R. J. Maqueda^{a)} and G. A. Wurden

Los Alamos National Laboratory, Los Alamos, New Mexico 87545

S. Zweben, L. Roquemore, H. Kugel, D. Johnson, and S. Kaye

Princeton Plasma Physics Laboratory, Princeton, New Jersey 08543

S. Sabbagh

Columbia University, New York, New York 10027

R. Maingi

Oak Ridge National Laboratory, Oak Ridge, Tennessee 37831

(Presented on 21 June 2000)

Turbulent filaments in visible light emission corresponding mainly to density fluctuations at the edge have been observed in large aspect ratio tokamaks: TFTR, ASDEX, Alcator C-Mod, and DIII-D. This article reports on similar turbulent structures observed in the National Spherical Torus Experiment (NSTX) using a fast-framing, intensified, digital visible camera. These filaments were previously detected mainly in high recycling regions, such as at limiters or antennas, where the line emission from neutral atoms was modulated by the fluctuations in local plasma density. However, by introducing controlled edge gas puffs, i.e., gas puff imaging, we have increased the brightness and contrast in the fluctuation images and allowed the turbulent structure to be measured independently of the recycling. A set discrete fiber-optically coupled sight-lines also measured the frequency spectra of these light fluctuations with a 200 kHz bandwidth. Initial results in NSTX show that the turbulent filaments are well aligned with the magnetic field which can be up to 45° from the horizontal at the outer midplane of NSTX. The dominant wavelength perpendicular to the magnetic field is ~7–11 cm, corresponding to a $k_{\perp} \rho_s$ of ~0.3 at an assumed $T_e = 25$ eV, and the frequency spectra has a typical broad shape characteristic of edge turbulence extending to about 100 kHz. By imaging a He gas puff along a magnetic field line the characteristic radial scalelength appears to be in the 3–5 cm range. © 2001 American Institute of Physics. [DOI: 10.1063/1.1321009]

I. INTRODUCTION

Edge turbulent filaments in visible light emission have been observed in large aspect ratio tokamaks: TFTR,^{1,2} ASDEX,³ Alcator C-Mod,⁴ and DIII-D.⁵ Edge turbulence in tokamaks and stellarators is believed to contribute to the radial flux of heat and energy across the separatrix and into the scrape off layer. As such it also affects the energy and particle deposition profiles on the divertor surfaces. This article describes initial measurements of the two-dimensional (2D) space-time structure of the edge turbulence as measured by a visible imaging diagnostic in the National Spherical Torus Experiment (NSTX).⁶ In the present work the contrast and brightness of the light fluctuation is increased by the introduction of a localized gas puff in the field of view of the imaging diagnostic, hence termed gas puff imaging (GPI). This approach is similar, although relatively simpler, than that employed in Ref. 5 where a neutral beam was employed to illuminate the turbulent eddies.

The characteristics of filamentary structure observed in the visible light emission from the plasma edge is similar to the edge density turbulent structure as measured with Langmuir probes.^{3,7} These filaments, normally seen in D_{α} emission, are highly elongated along the magnetic field ($\lambda \gg 1$ m

long), but have a short scale length across the field in the poloidal direction ($\lambda_{\perp} \approx 1-10$ cm). These light fluctuations are thought to be due to the rapid excitation of the neutral atoms by the electron density fluctuations, i.e., $S \propto n_0 n_e f(T_e)$, where S is the local light emission from neutrals, n_0 is the local neutral density (assumed not to fluctuate on fast time scales), n_e is the local electron density, and $f(T_e)$ is normally a weak function within some range of edge temperatures. The fluctuation characteristics in S and n_e (as measured by a Langmuir probe) were shown to be similar on ASDEX³ and on the Caltech tokamak⁷ and, under low density conditions, the light emission intensity of the He I line at 587.6 nm was calculated to be proportional to the electron density responsible for its excitation.⁴ The average electron density in NSTX is below $3 \times 10^{19} \text{ m}^{-3}$ and lower at the edge. Thus we take as a working assumption that the structure of the visible light emission from the plasma edge is approximately the same as the structure of the edge density turbulence.

Two images obtained in NSTX with a 20 μs exposure and 1 ms apart in time can be seen in Fig. 1. The filament structure can be clearly seen over the high harmonic fast wave (HHFW) antenna (90 cm high). In this case the turbulence is “illuminated” by the natural recycling from the antenna’s Faraday shield. This introduces the complication that the characteristics of the light emission from the neutral at-

^{a)}Electronic mail: maqueda@lanl.gov

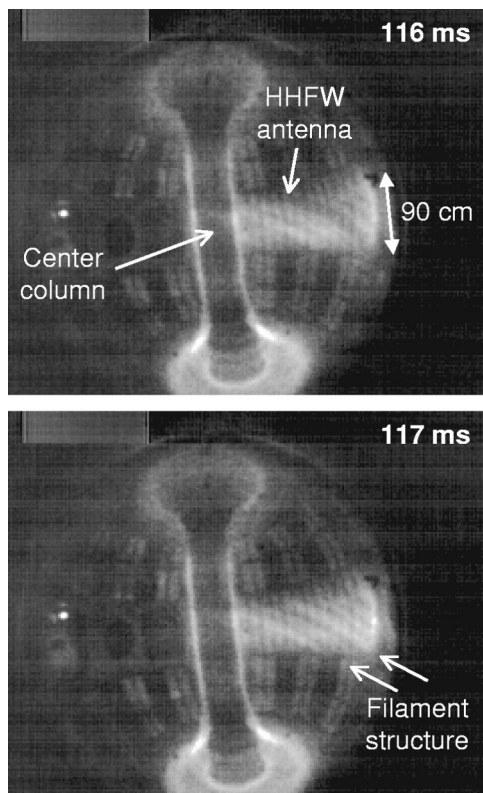


FIG. 1. Edge turbulent filaments observed over the HHFW antenna “illuminated” by natural recycling from the Faraday shield. Images obtained with $20 \mu\text{s}$ exposure and no interference filter (discharge 101125).

oms is not only modulated by the fluctuations in the local electron density but depends on the recycling level. For instance, it has been observed at Alcator C-Mod that the filamentation diminishes considerably during *H*-mode confinement phases in comparison with *L*-mode.⁸ This is due almost exclusively to the lower recycling level characteristic of this higher confinement regime. Essentially no differences are observed in the scrape-off layer turbulence in Alcator C-Mod when plasmas with *H*-mode are compared with those *L*-mode confinement.⁴ This is where gas puff imaging introduces one more advantage over the observation of natural recycling: by GPI the turbulent structure can be measured independently of the recycling.

II. GAS PUFF IMAGING

The visible light emission structure in NSTX is measured using a fast-framing camera diagnostic, used previously on TFTR.² This diagnostic is based on an intensified Kodak Ektapro digital camera capable of acquiring full images (239×192 pixels) at a 1000 Hz frame rate. The digitization of each pixel is 8 bit deep. The new feature of the edge turbulence measurements in NSTX, as mentioned above, is the use of gas puff imaging, i.e., the use of a local gas puff in the camera field of view to increase the local neutral density n_0 and thus the brightness (and contrast) of the fluctuation images. The images in NSTX were produced by either filtered D_α or He I (587.6 nm) light, or total visible light (440–700 nm). The views of the edge turbulent structure were either the poloidal versus toroidal or poloidal ver-

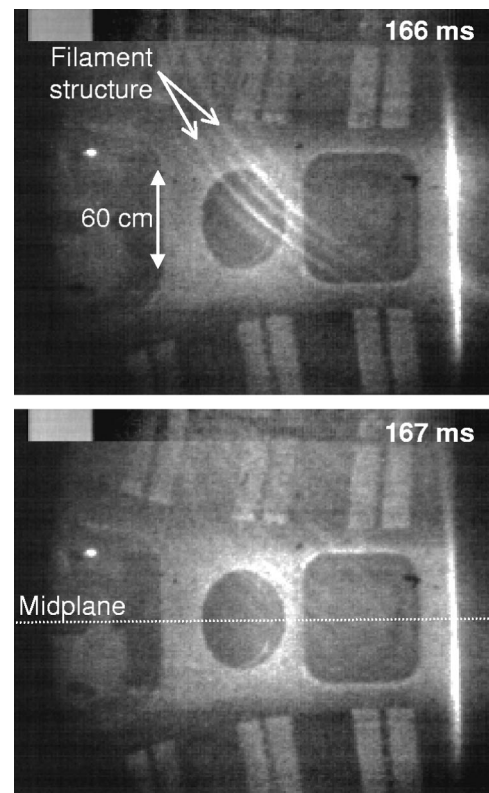


FIG. 2. Images of the edge turbulence in the poloidal vs toroidal plane. Images obtained with $10 \mu\text{s}$ exposure and no interference filter. The high recycling layer over the center column can be seen close to the right edge of these images (discharge 101533).

sus radial planes. In this later case the localized gas puff is set so that the turbulent structure is viewed along a magnetic field line. Since the characteristic wavelength along the field line is long this then yields images of “eddy”-like structures.

Since the turbulence autocorrelation time is much faster than the framing rate of the fast camera (1 frame/ms), a supplementary measurement of the time dependence of the edge turbulence was made in NSTX using a set of discrete fiber-optically coupled sight-lines. Each sight-line was focused onto a 4–5 cm diam within the gas puff and detected using a photomultiplier tube with a bandwidth of ~ 200 kHz, and sampled at 500 kHz.

III. INITIAL RESULTS

Two consecutive images (frame rate of 1 kHz) of the outer midplane edge region of NSTX can be observed in Fig. 2. These images were obtained with a $10 \mu\text{s}$ long exposure and no interference filter. In Fig. 2, the edge turbulent filaments are illuminated by a deuterium gas puff from the 60 cm diam circular port in the middle of the image. These filaments are aligned nearly along the magnetic field, which had an $\sim 42^\circ$ angle to the toroidal direction at the midplane in this $I = 0.8$ MA, $B = 0.3$ T case (as evaluated by EFIT), and have a broad range of poloidal wavelengths centered at $\lambda_\perp \sim 10$ –15 cm. In the case of Fig. 1 the angle of the filaments is closer to 30° due to the lower plasma current ($I = 0.5$ MA). In views such as these, the filamentary structure

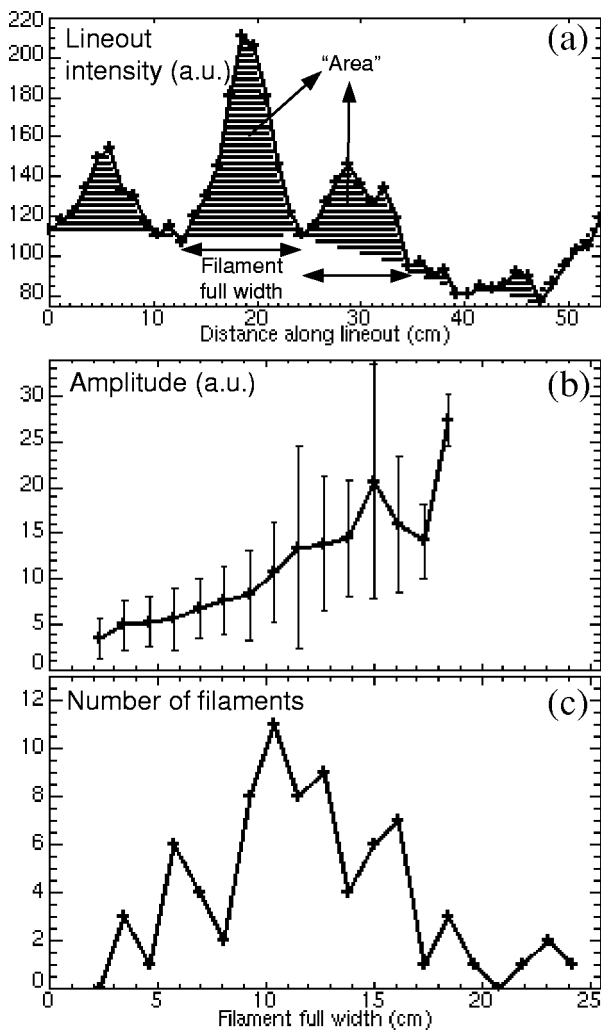


FIG. 3. Spatial characteristics of the turbulent filaments. (a) Poloidal lineout on gas puff in discharge 101533 at 166 ms. The “filament full width” and “area” of the filament are defined. (b) Filament amplitude, defined as area/full width, as a function of the width. The filament amplitude increases with its width. (c) Distribution of the filament widths for the filaments with amplitude ≥ 13 . The distribution of the brightest filaments is centered on 10–15 cm.

disappears at exposure times above $\sim 100 \mu\text{s}$ and there is no repeated spatial structure from one frame to the next.

The dominant poloidal wavelength is $\lambda_{\text{pol}} \sim 10\text{--}15 \text{ cm}$ near the outer midplane, based on the analysis of many poloidal versus toroidal images such as those in Fig. 2. Figure 3 shows the distribution of the filament full width as defined in Fig. 3(a). It is seen in this figure that the fluctuation amplitude (=area/width) appears to increase with the filament width [Fig. 3(b)]. Figure 3(c) shows that the width distribution is broadband, peaking in the 10–15 cm range for the brightest filaments.

This poloidal wavelength of 10–15 cm is equivalent to a wavelength perpendicular to the field of $\lambda_{\perp} \sim 7\text{--}11 \text{ cm}$ which is up to a factor of 2 larger than the $\lambda_{\perp} \sim 5 \pm 2 \text{ cm}$ observed for the visible light filaments on the inner limiter of TFTR at $B \sim 8 \text{ T}$,¹ or the $\lambda_{\perp} \sim 6 \pm 2 \text{ cm}$ observed near the outer edge on ASDEX at $B \sim 2 \text{ T}$.³ This suggests that the perpendicular wavelength of edge turbulence is not very sensitive to the magnetic field strength. In the NSTX case one

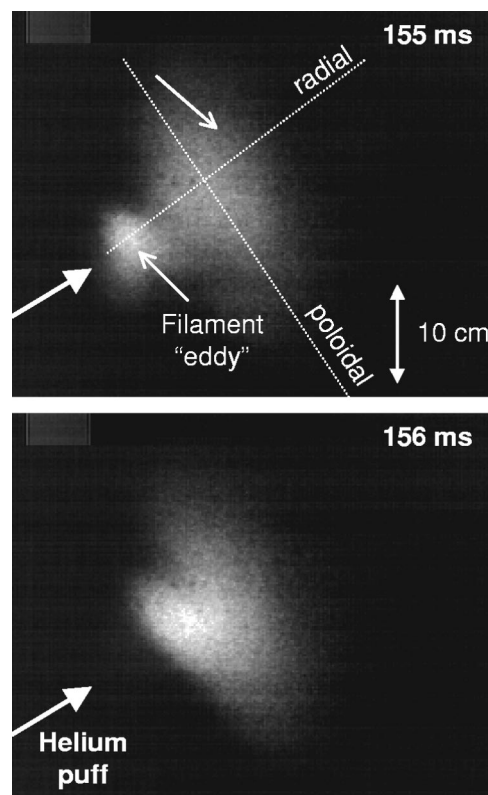


FIG. 4. Images of the edge turbulence in the poloidal vs radial plane. Images obtained with $10 \mu\text{s}$ exposure and a He I interference filter (587.6 nm). The approximate location of the helium gas puff is indicated by arrows. The turbulence is seen as rapidly changing “eddies” with radial scalelengths of 3–5 cm (discharge 101989).

can estimate $k_{\perp} \rho_s \approx 0.3$ (with $\lambda_{\perp} = 7\text{--}11 \text{ cm}$ at an assumed $T_e = 25 \text{ eV}$ for the local $B = 0.15 \text{ T}$).

The poloidal versus radial structure of the visible light emission from a helium gas puff just near the separatrix 50 cm above the outer midplane is shown in Fig. 4. In this case a He I line filter at 587.6 nm is used with $10 \mu\text{s}$ exposures. The observed spatial structure has a large variation from frame-to-frame over the $15 \text{ cm} \times 15 \text{ cm}$ approximate area illuminated by the puff, such as seen in the difference between the two consecutive frames shown (1 ms apart). The poloidal scale of these filaments is consistent to that seen in Figs. 1 and 2: at most only one turbulent eddy can be observed in any one frame. The radial scalelength of the light emission, on the other hand, is observed to be in the 3–5 cm range. The size of the light emission due to the gas puff is comparable to the poloidal scale of the turbulence yielding at most one eddy within the puff. Consequently, it is difficult to characterize the radial size spectrum, except to say that there does not appear to be structure on the scale of $\sim 1 \text{ cm}$ (which should have been resolvable in these images).

Figure 5 shows an output from a discrete channel detector which viewed a 5 cm diam area within the 60 cm diam gas puffing port shown in Fig. 2. The raw signals, as shown in Figs. 5(a) and 5(b), typically have a fluctuation level of (rms/mean) $\sim 25\%$, with a typical autocorrelation time of $\leq 40 \mu\text{s}$ seen Fig. 5(d). The frequency spectrum [Fig. 5(e)] is similar to other measurements of edge turbulence.⁹ There

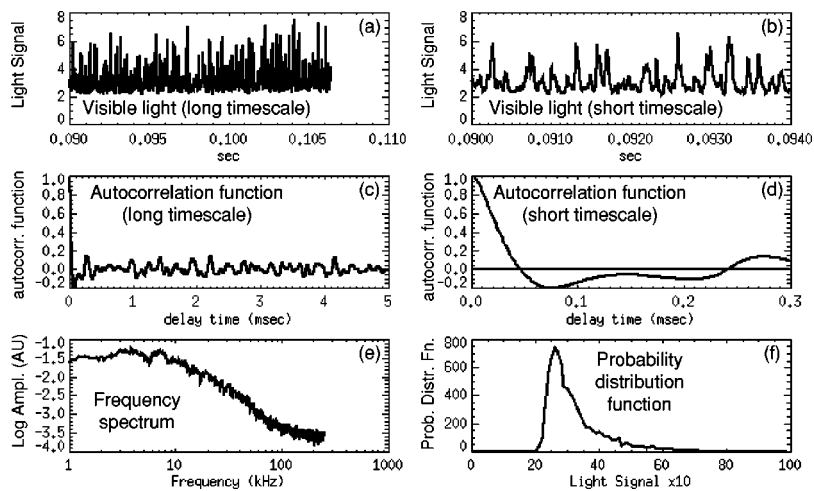


FIG. 5. Time series analysis of the visible light signal from a discrete channel viewing the gas puff shown in Fig. 2 (discharge 101585). These signals are similar that of edge density turbulence observed in other devices.

appears to be some “bursting” in the raw signal, as shown in Fig. 5(b) and also seen in the skewed probability distribution function in Fig. 5(f). However, there are apparently no significant long-time tails of the autocorrelation function, e.g., as in Figs. 5(c) and 5(d), except during occasional low frequency coherent MHD activity. The signals observed in Fig. 5 are similar to edge turbulence observed in other toroidal devices; for example, the frequency spectrum in Fig. 5(e) is similar to that seen with Langmuir probes in the large JET tokamak,⁹ and also that observed recently in Alcator C-Mod using visible light emission from a helium gas puff.⁴ This reinforces the idea that the edge turbulence does not depend sensitively on the size or magnetic field of the tokamak.

IV. DIAGNOSTIC AND ANALYSIS DEVELOPMENT

The gas puff imaging diagnostic described in this article has started to provide useful insights on the edge turbulence observed in NSTX. Nevertheless improvements are required in the hardware together with further development of the analysis. The localized gas puff used in the poloidal versus radial view of the turbulence was limited in size and hence yielded only limited scale-length information on the turbulent filaments (seen as eddies when observed along the magnetic field line). A poloidally extended gas puff manifold has been installed in NSTX to increase the poloidal range of this system while still maintaining a short gas puff dimension in the toroidal direction.

Further quantitative interpretation of the images obtained requires a detailed model for the local relationship between the edge density fluctuations and the visible light fluctua-

tions, which depends upon the atomic physics of the light emission process, the neutral penetration physics, and the effect of possible electron temperature and neutral density fluctuations. The turbulence wavelength sensitivity needs to be evaluated for each configuration to take into account the averaging over small wavelengths and the undersampling of large wavelengths. Finally, the possible effect of large neutral gas puffs on the edge turbulence needs to be evaluated both theoretically and experimentally. Based on this modeling, the results of visible imaging of edge turbulence can be quantitatively compared with the recent numerical models for edge turbulence.^{10–12}

ACKNOWLEDGMENTS

The authors wish to thank W. Blanchard for his invaluable assistance in setting up the gas puff system required for this work. This work was supported by the U.S. Department of Energy under Contract Nos. W-7405-ENG-36 and DE-AC02-CHO3073.

¹S. J. Zweben and S. S. Medley, *Phys. Fluids* **B1**, 2058 (1989).

²R. Maqueda and G. Wurden, *Nucl. Fusion* **39**, 629 (1999).

³M. Endler *et al.*, *Nucl. Fusion* **35**, 1307 (1995).

⁴J. L. Terry, in *Proceedings 14th International Conference on Plasma-Surface Interactions in Controlled Fusion Devices*, Rosenheim, Germany, 2000.

⁵R. Fonck, *Phys. Plasmas* (to be published).

⁶S. M. Kaye *et al.*, *Fusion Technol.* **36**, 16 (1999).

⁷S. J. Zweben and R. Gould, *Nucl. Fusion* **23**, 825 (1983).

⁸D. Hübner *et al.*, *Bull. Am. Phys. Soc.* **44**, 208 (1999).

⁹M. Endler, *J. Nucl. Mater.* **266–269**, 84 (1999).

¹⁰B. N. Rogers and J. F. Drake, *Phys. Rev. Lett.* **79**, 229 (1997).

¹¹F. Jenko and B. D. Scott, *Phys. Plasmas* **6**, 2705 (1999).

¹²X. Q. Xu *et al.*, *Phys. Plasmas* **7**, 1951 (2000).